Inorganic Chemistry

ARTICLE

pubs.acs.org/IC

Reactions of the Bis(dialkylphosphino)methane Complexes $Pd_2X_2(\mu\text{-}R_2PCH_2PR_2)_2$ (X = halogen, R = Me or Et) with H_2S, S_8, COS, and CS_2; Detection of Reaction Intermediates

Craig B. Pamplin, Steven J. Rettig,[†] Brian O. Patrick, and Brian R. James*

Department of Chemistry, University of British Columbia, Vancouver, British Columbia, Canada V6T 1Z1

Supporting Information

ABSTRACT: The $Pd_2X_2(dmpm)_2$ complexes [X = Cl (**1a**), Br (**1b**), I (**1c**); dmpm = bis(dimethylphosphino)methane. In all the dipalladium complexes mentioned in this paper, the dmpm, depm, and dppm ligands (unless stated otherwise) are bridging, but for convenience the μ-symbol is omitted.] react with H_2S to yield H_2 and the bridged-sulfido complexes $Pd_2X_2(\mu\text{-}S)(dmpm)_2$ (**2a**−**c**), of which **2a** and **2b** are structurally characterized. With **1a**, two rapid reversible equilibria are observed by NMR spectroscopy below −30 °C, and two reaction intermediates are detected; both are likely hydrido(mercapto) species. Reaction of **1a** with 1 equiv of elemental sulfur also yields **2a**. The reaction of **1a** with COS results in the initial formation of $Pd_2Cl_2(\mu\text{-}COS)(dmpm)_2$ (**3**) that undergoes decarbonylation to yield **2a** and $Pd_2Cl_2(\mu\text{-}CO)(dmpm)_2$ (**4**), which is also formed via reversible insertion of the CO into the Pd−Pd bond of **1a**. The solid-state molecular structure of the previously reported complex $Pd_2Cl_2(\mu\text{-}CS_2)(dmpm)_2$ (**5**), together with solution NMR data for **3** and **5**, reveal that the bridging heterocumulene ligands coordinate in an η^2-*C,S* fashion. Analogous findings were made for the corresponding $Pd_2X_2(depm)_2$ complexes [X = Cl (**1a′**), Br (**1b′**), I (**1c′**); depm = bis(diethylphosphino)methane], although no μ-COS species was detected. The $Pd_2X_2(\mu\text{-}S)(depm)_2$ complex was structurally characterized. Differences in the chemistry of the previously studied, corresponding dppm systems (dppm = bis(diphenylphosphino)methane) are discussed.

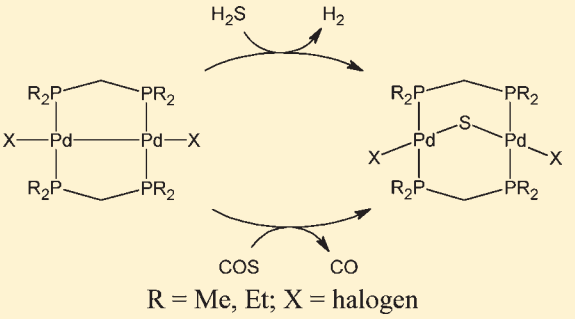

INTRODUCTION

Bidentate tertiary phosphine ligands such as bis(diphenylphosphino)methane (dppm) and bis(dimethylphosphino)methane (dmpm) have been used extensively for the stabilization of di- and trinuclear metal complexes and metal clusters.[1] The versatile coordination chemistry of dppm in particular becomes apparent within dipalladium complexes, where the so-called side-by-side,[2] A-frame,[3,4] face-to-face[5] and so-called manxane-type[6] geometries have been characterized. The coordination chemistry and reactivity of these and related complexes are markedly dependent on the steric and electronic characteristics of the diphosphine ligand, and steric factors in particular play a crucial role in determining the nuclearity of the complexes. For example, the smaller and more electron-rich dmpm ligand stabilizes the face-to-face, isolable *trans*-$Pd_2X_4(dmpm)_2$ (X = halogen atom) or a $Pd_2I_2(\mu\text{-}I)_2(dmpm)_2$ complex,[7] while the corresponding dppm species spontaneously convert to the monomeric $PdX_2(dppm)$ complexes (Scheme 1).[8,9] Of note, the face-to-face $Pd_2Cl_2Me_2(dmpm)_2$ complex, prepared by treating $Pd_2Me_4(dmpm)_2$ with 2 equiv of HCl[10] or by reaction of PdCl(Me)(COD) with dmpm,[11] reacts with silica to afford an efficient heterogeneous catalyst for the cyclization of aminoalkynes,[10] and exemplifies the potential catalytic activity of Pd-dmpm systems.

The studies presented here stem from previous reports from our group that have described the stoichiometric reaction of $Pd_2X_2(dppm)_2$ with H_2S in CH_2Cl_2 to generate $Pd_2X_2(\mu\text{-}S)(dppm)_2$ and H_2 (eq 1), as well as an associated catalytic conversion of H_2S and dppm to H_2 and the monosulfide dppm(S).[12] Low temperature NMR and kinetic studies revealed the presence of the "face-to-face" hydrido-sulfhydryl intermediates,

$$Pd_2X_2(dppm)_2 + H_2S \rightarrow Pd_2X_2(\mu\text{-}S)(dppm)_2 + H_2 \quad (1)$$

$Pd_2X_2(H)(SH)(dppm)_2$, formed via oxidative addition of H_2S across the Pd−Pd bond of $Pd_2X_2(dppm)_2$, but no precursor H_2S adduct was detected.[12] The extension of the studies to the corresponding dmpm systems was initiated by knowledge of the water-solubility of $Pd_2Cl_2(dmpm)_2$[13] and the possibility of extending the chemistry to aqueous systems.[7] However, it soon became obvious that the nonaqueous chemistry of the dmpm system was noticeably different from that of the dppm system, particularly in the low temperature detection of further intermediates; the possibility of an initially formed H_2S-adduct prompted us to pursue this nonaqueous chemistry especially the reactions of $Pd_2Cl_2(dmpm)_2$ (**1a**) with the sulfur-containing molecules, H_2S, S_8, COS, and CS_2. The heterocumulene

Received: March 11, 2011
Published: July 22, 2011

Scheme 1. Structural Variation in Pd^{II}-Diphosphine Halogen Complexes[a]

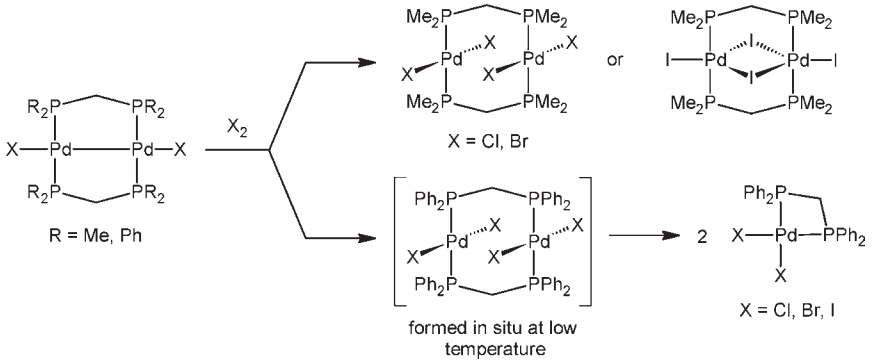

[a] X = halogen.

molecules, although unreactive toward $Pd_2Cl_2(dppm)_2$, generated some novel chemistry with the bis(dialkylphosphino)methane analogues.

Subsequent to our first report on the chemistry of reaction 1,[14] other reports have described the reaction of H_2S with several heterobinuclear dppm complexes of the type $MM'(CO)_n(dppm)_2$ (n = 3−5), where M and M′ may be the same or different transition metals, including a report from our group on the $MoRu(CO)_6(dppm)_2$ system.[15]

Such chemistry, particularly within Pd systems, is of interest because of the "poisoning" effect of H_2S (and, to a lesser extent, COS and sulfur) on heterogeneous, Group 10 metal catalysts that effect hydrogenation, dehydrogenation, steam-reforming and hydrocracking.[16a] More generally, interaction of transition metal complexes with H_2S is relevant in biological sulfur cycles and cytotoxicity, the formation of ores, and in hydrodesulfurization catalysis.[12a,16b]

RESULTS AND DISCUSSION

Reactions of $Pd_2X_2(dmpm)_2$ Complexes [X = Cl (1a), Br (1b), I (1c)] with H_2S and with S_8. Yellow-orange solutions of **1a** or **1b** in CH_2Cl_2 at room temperature rapidly turn red upon exposure to 1 atm of H_2S as the bridged-sulfido complexes $Pd_2X_2(\mu\text{-}S)(dmpm)_2$ [X = Cl (**2a**), Br (**2b**)] are formed; the H_2 produced is readily detected at δ 4.58 (in CD_2Cl_2) The orange-brown iodo analogue (**2c**) can be made similarly within a much slower reaction ($t_{1/2}$ of ∼2 h), but is more readily formed from the diphosphine exchange reaction of the violet $Pd_2I_2(\mu\text{-}S)(dppm)_2$ with dmpm in CH_2Cl_2. The complexes **2a**−**c** are readily isolated in >90% yields, and are well characterized by elemental analysis and NMR spectroscopy and, in the case of **2a**, by X-ray crystallography (Figure 1, Tables 1−3). The reaction of **1a** with excess D_2S in CD_2Cl_2 gave clean formation of **2a** and D_2, and there was no evidence for incorporation of deuterium into the dmpm ligand. Complex **2a** was isolated also from treatment of **1a** with either COS (see below), or elemental sulfur in a 1:1 Pd:S reaction.

In **2a**, the nonbonding Pd···Pd distance of 3.342 Å is greater than those found in $Pd_2Cl_2(\mu\text{-}S)(dppm)_2$ and $Pd_2Cl_2(\mu\text{-}CO)(dmpm)_2$ (3.258[17] and 3.171 Å,[18] respectively) and related Pd^{II} A-frame complexes.[1b,c] Consistent with the longer Pd···Pd distance, the Pd−S−Pd angle (93.77°) is slightly more obtuse, and the average Pd−S bond length (2.289 Å) slightly shorter, than

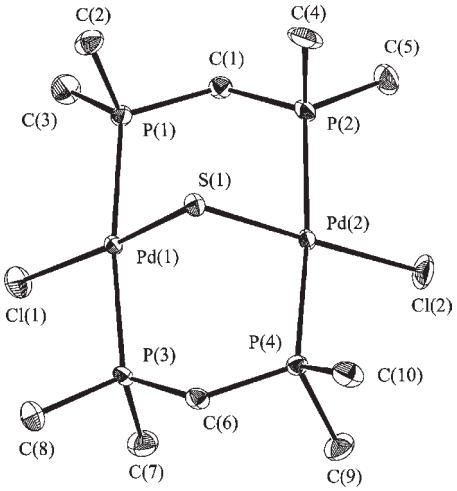

Figure 1. ORTEP diagram of $Pd_2Cl_2(\mu\text{-}S)(dmpm)_2$ (**2a**) with thermal ellipsoids shown at the 50% probability level.

those found in $Pd_2Cl_2(\mu\text{-}S)(dppm)_2$ (90.3(2)° and ∼2.298 Å); the Pd−P and Pd−Cl bond distances are within 0.05 Å of those seen for the dppm analogue.[17] Like other structurally characterized A-frame dmpm complexes containing chloro ligands,[18,19] the $Pd_2P_4C_2$ ring of **2a** adopts a chair conformation in the solid state, with the methylene C-atom of one dmpm ligand oriented toward the apical sulfide ligand (cf. **2b** below): this means that each of the four methylene H-atoms are inequivalent. In contrast, the dppm analogue and most other dppm-bridged A-frame complexes adopt a boat conformation with both the CH_2 groups directed toward the bridging ligand to minimize steric interactions between adjacent Ph groups.[1b,c,2−4] Rare exceptions to this generality include $Pd_2(OCOCF_3)_2(\mu\text{-}CO)(dppm)_2$,[20] which crystallizes in a distorted chair conformation, and $[Pd_2R_2(\mu\text{-}Br)(dppm)_2]PF_6$ (R = mesityl),[21] in which the ring conformation is a boat with the CH_2 groups bent *away* from the bridging bromo ligand. In the structure of **2b** (Figure 2, Tables 1−3), the Pd···Pd distance of 3.072 Å is significantly shorter than that in **2a**; this and the severe twisting within the $Pd_2P_4C_2$ ring result from the larger covalent radii of the Br ligands (1.14 vs 0.99 Å for Cl).[22] When viewed down the Pd···Pd vector, the two P−Pd−P axes in **2b** are mutually twisted ∼30°, while those in **2a** are virtually parallel, and the $Pd_2P_4C_2$ ring conformation in **2b** is thus best described as

dx.doi.org/10.1021/ic200503d |*Inorg. Chem.* 2011, 50, 8094–8105

Table 1. Crystallographic Data for $Pd_2Cl_2(\mu\text{-}S)(dmpm)_2$ (2a), $Pd_2Br_2(\mu\text{-}S)(dmpm)_2$ (2b), and $Pd_2Cl_2(\mu\text{-}CS_2)(dmpm)_2$ (5)

	2a	2b	5
empirical formula	$C_{10}H_{28}Cl_2P_4Pd_2S$	$C_{10}H_{28}Br_2P_4Pd_2S$	$C_{11}H_{28}Cl_2P_4Pd_2S_2$
fw	587.96	676.88	683.49
color, habit	red, prism	red, prism	red, irregular
cryst size, mm	0.30 × 0.33 × 0.38	0.50 × 0.40 × 0.30	0.30 × 0.35 × 0.40
cryst system	orthorhombic	monoclinic	trigonal
space group	$P2_12_12_1$ (#19)	$P2_1$ (#4)	$R\bar{3}$ (#148)
a (Å)	10.9707(11)	8.2224(10)	27.7975(4)
b (Å)	12.3132(3)	8.3638(14)	27.7975(4)
c (Å)	15.2999(2)	15.8628(4)	17.7113(5)
β (deg)	90	93.9050(10)	90
V (Å^3)	2066.8(2)	1088.4(2)	11852.0(4)
Z	4	2	18
D_{calc} (g/cm^3)	1.890	2.065	1.724
μ, cm^{-1}	23.96	57.01	20.37
total reflns	17706	9314	35236
unique reflns	5278	4613	7381
R_{int}	0.0215	0.0421	0.000
no. of variables	180	181	198
$R(F)$ $(I \geq 2\sigma(I))^a$	0.0175	0.0364	0.0274
$R_w(F^2)$ (all data)^a	0.0439	0.0906	0.0750
GOF	1.085	1.152	1.119
residual density, e/Å^3	−0.735	−1.773	−0.880

^{a} Function minimized $\Sigma w(F_o^2 - F_c^2)^2$, where $w = 1/\sigma^2(F_o^2)$; $R = \Sigma||F_o^2| - |F_c^2||/\Sigma|F_o^2|$, and $R_w = \Sigma w(|F_o^2| - |F_c^2|)^2/\Sigma wF_o^4]^{1/2}$.

Table 2. Selected Bond Lengths (Å) with Estimated Standard Deviations in Parentheses

	$Pd_2Cl_2(\mu\text{-}S)(dmpm)_2$ (**2a**)		
Pd(1)···Pd(2)	3.3419(2)	Pd(1)−P(1)	2.2930(6)
Pd(1)−Cl(1)	2.3645(6)	Pd(1)−S(1)	2.2895(6)
Pd(2)−Cl(2)	2.3605(6)	Pd(2)−S(1)	2.2884(6)
	$Pd_2Br_2(\mu\text{-}S)(dmpm)_2$ (**2b**)		
Pd(1)···Pd(2)	3.0719(5)	Pd(1)−P(1)	2.2857(15)
Pd(1)−Br(1)	2.4951(7)	Pd(1)−S(1)	2.3046(15)
Pd(2)−Br(2)	2.4813(7)	Pd(2)−S(1)	2.3057(14)
	$Pd_2Cl_2(\mu\text{-}CS_2)(dmpm)_2$ (**5**)		
Pd(1)···Pd(2)	3.0883(3)	Pd(2)−C(11)	1.974(2)
Pd(1)−Cl(1)	2.3383(7)	Pd(1)−S(1)	2.3143(6)
Pd(2)−Cl(2)	2.4023(6)	S(1)−C(11)	1.708(3)
Pd(1)−P(1)	2.3145(7)	S(2)−C(11)	1.651(2)

an extended boat. Subtle steric effects introduced by halide (or pseudohalide) ligands in such complexes may well play a role in their reactivity because of the structural rearrangements that accompany, for example, A-frame formation.

Solution ^{1}H and ^{1}H{^{31}P} NMR spectra of **2a** (and **2b**), however, show only two diastereotopic methylene protons, each appearing as a doublet of quintets because of geminal $^2J_{HH}$ coupling and "virtual coupling" to four equivalent ^{31}P nuclei. For **2c**, one of the quintets is not clearly identified because of overlap

Table 3. Selected Bond Angles (deg) with Estimated Standard Deviations in Parentheses

	$Pd_2Cl_2(\mu\text{-}S)(dmpm)_2$ (**2a**)		
Pd(1)−S(1)−Pd(2)	93.77(2)	P(1)−Pd(1)−P(3)	172.41(2)
Cl(1)−Pd(1)−S(1)	174.27(2)	Pd(1)−P(1)−C(1)	113.01(7)
Cl(1)−Pd(1)−P(1)	95.96(2)	Pd(1)−P(1)−C(3)	116.03(10)
Cl(1)−Pd(1)−P(3)	89.60(2)	P(1)−C(1)−P(2)	120.02(13)
S(1)−Pd(1)−P(1)	83.46(2)	S(1)−Pd(1)−P(3)	91.51(2)
	$Pd_2Br_2(\mu\text{-}S)(dmpm)_2$ (**2b**)		
Pd(1)−S(1)−Pd(2)	83.57(5)	P(1)−Pd(1)−P(3)	173.12(5)
Br(1)−Pd(1)−S(1)	173.78(4)	Pd(1)−P(1)−C(1)	111.1(2)
Br(1)−Pd(1)−P(1)	97.45(4)	Pd(1)−P(1)−C(3)	116.9(3)
Br(1)−Pd(1)−P(3)	88.99(4)	P(1)−C(1)−P(2)	113.8(3)
S(1)−Pd(1)−P(1)	80.68(6)	S(1)−Pd(1)−P(3)	92.67(6)
	$Pd_2Cl_2(\mu\text{-}CS_2)(dmpm)_2$ (**5**)		
S(1)−C(11)−S(2)	123.15(14)	P(1)−Pd(1)−P(3)	177.40(3)
Pd(2)−C(11)−S(1)	113.48(12)	P(2)−Pd(2)−P(4)	173.34(2)
Pd(2)−C(11)−S(2)	123.37(14)	S(1)−Pd(1)−P(1)	85.57(2)
Pd(1)−S(1)−C(11)	103.44(8)	P(2)−Pd(2)−C(11)	86.51(7)
Cl(1)−Pd(1)−S(1)	176.05(3)	S(1)−Pd(1)−P(3)	92.95(2)
Cl(2)−Pd(2)−C(11)	177.79(7)		

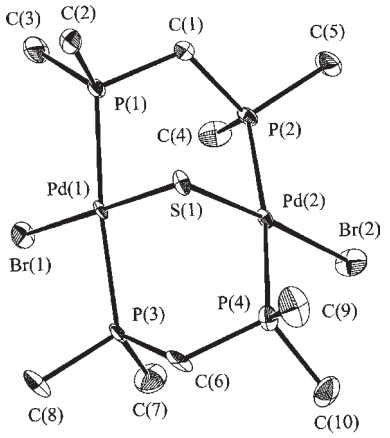

Figure 2. ORTEP diagram of $Pd_2Br_2(\mu\text{-}S)(dmpm)_2$ (**2b**) with thermal ellipsoids shown at the 50% probability level.

with the CH_3 signals, which for all three complexes are seen in the δ 1.85−1.60 region. The dynamic process capable of exchanging geminal methylene hydrogen sites most likely involves a rapid conformational equilibrium between the chair and boat isomers, with the CH_2 groups "flipping" rapidly from one side of the $Pd_2P_4C_2$ ring plane to the other; although such fluxionality is incapable of exchanging the geminal PCH_2P proton resonances,[17] it does render the two dmpm ligands equivalent by symmetry, even at −90 °C (tested for **2a**). The ^{31}P{^{1}H} NMR spectra of **2a**−**c** appear as a singlet in the δ −10 to −16 region, even at the lowest accessible temperatures (i.e., −120 °C in $CDFCl_2$). Similar solution NMR spectra are seen for the corresponding $Pd_2X_2(\mu\text{-}S)(dppm)_2$ complexes.[17,23]

Consistent with the synthesis of **2c** by the ligand exchange reaction of $Pd_2I_2(\mu\text{-}S)(dppm)_2$ with dmpm, a CH_2Cl_2 solution of **2c** was stable in the presence of dmpm or dppm, and no phosphine sulfides were detected. Similarly, **2a** and **2b** do not

react with these diphosphines. In contrast, addition of dppm to solutions of $Pd_2X_2(\mu\text{-}S)(dppm)_2$ results in abstraction of the sulfur and formation of dppm(S) with regeneration of $Pd_2X_2(dppm)_2$, chemistry that results in the catalytic conversion of H_2S into H_2 and dppm(S).[12,23] Presumably the higher basicity of the dmpm ligands in the $Pd_2X_2(\mu\text{-}S)(dmpm)_2$ complexes (vs that in the dppm analogues) nullifies reactivity of the bridged sulfide toward an incoming nucleophilic P-atom of the chelating diphosphine.[23] The extraction of a sulfide ligand by a phosphine is well documented,[12,23−25] and an example with dmpm is its reaction with $[MeRe(NAr)_2]_2(\mu\text{-}S)_2$ (Ar = 2,6-diisopropylphenyl) to yield dmpm(S) and $[MeRe(NAr)_2]_2(\mu\text{-}S)$ or $MeRe(NAr)_2(\eta^1\text{-}dmpm)_2$, depending on the phosphine concentration used.[25]

Reactions of $Pd_2X_2(depm)_2$ Complexes [X = Cl (1a′), Br (1b′), I (1c′)] with H_2S and with S_8. The well characterized $Pd_2Cl_2(\mu\text{-}S)(depm)_2$ complex (**2a′**) was readily isolated from the reaction of $Pd_2X_2(depm)_2$ (**1a′**) in CH_2Cl_2 with H_2S or with S_8. Reactions of $Pd_2X_2(depm)_2$ [X = Br (**1b′**), I (**1c′**)] with H_2S similarly generate in situ **2b′** or **2c′**, respectively, and H_2 as determined by NMR spectroscopy (in CD_2Cl_2), but the reactions are slow, and **2b′** and **2c′** were more conveniently obtained in ∼75% isolated yields from the halide metathesis reactions of **2a′** with NaX (X = Br, I); the complexes were characterized by ^1H and $^{31}P\{^1H\}$ NMR spectroscopy and elemental analysis.

Variable-Temperature NMR Studies on the H_2S Reactions. As noted in the Introduction, $Pd_2X_2(H)(SH)(dppm)_2$ species were detected in earlier studies on the $H_2S/Pd_2X_2(dppm)_2$ systems, and kinetic data were consistent with reductive elimination of H_2 from this species with coformation of the μ-S product (cf. eq 1).[12] Low temperature NMR experiments were carried out on the currently studied $Pd_2Cl_2(dmpm)_2$ (**1a**) and $Pd_2Cl_2(depm)_2$ (**1a′**) systems with the hope of detecting a presumed, initially formed H_2S complex; our findings do indeed reveal several intermediates, but there is no convincing evidence for an H_2S-adduct. To the best of our knowledge, there are no reports of any Pd−H_2S species, and more generally structurally characterized H_2S complexes remain few in number.[12a,26]

The fluxionality of the $Pd_2X_2(dmpm)_2$ and $Pd_2X_2(depm)_2$ complexes has been described previously[7,27] and, for example, the ^1H NMR spectrum of a solution of **1a** in CD_2Cl_2 at −80 °C exhibits a broad quintet at δ 2.66 for the CH_2 protons, and signals at δ 1.34 and 1.81 for the two diastereotopic methyl groups; the $^{31}P\{^1H\}$ resonance appears as a singlet at δ −29.8 throughout the temperature range −90 to +30 °C. On addition of H_2S (1.0 equiv) via a microsyringe to the septum-sealed NMR tube at −80 °C, the gas condenses on the walls of the tube and dissolves when the tube is shaken. There is no color change, yet partial formation of new species is detected: the major species shows an ABCD pattern in the $^{31}P\{^1H\}$ spectra (Figure 3) with the main resonances at δ −10.4, −4.9, −9.5, and −3.7, while the minor species gives rise to a less intense AA′BB′ pattern with resonances centered at δ −5.4 and −6.4. The ABCD pattern is attributed to a species labeled **A**, while the AA′BB′ signal is attributed to species **B**. Identical signals are observed when six equivalents of H_2S were used, and the singlet resonance of **1a** was only slightly diminished, while the ABCD and AA′BB′ signals slightly increased in intensity.

Warming the solution to −40 °C results in the reversible coalescence of both sets of $^{31}P\{^1H\}$ signals that now appear as pseudotriplet AA′BB′ patterns at δ −4.6 and −10.1 (for **A**) and a broad peak at δ ∼7 (for **B**), the fluxionality of **A** and **B** being

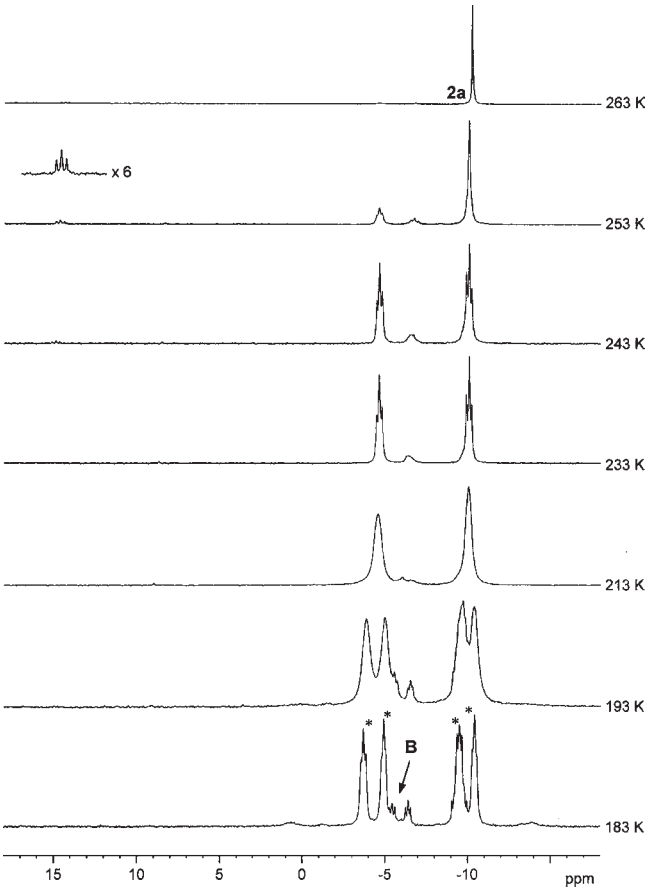

Figure 3. Variable temperature $^{31}P\{^1H\}$ NMR spectra (121.5 MHz, CD_2Cl_2) on addition of H_2S (1.0 equiv) to $Pd_2Cl_2(dmpm)_2$ (**1a**) at lower temperatures. The ABCD pattern attributed to **A** is labeled with asterisks; the singlet of **1a** (δ −29.8) is not shown.

apparent from the coalescence behavior. Repeated cycling of the temperature between −90 and −40 °C consistently regenerates these characteristic signals, and no evolution of H_2 is observed under these conditions (see below). From −30 to −20 °C, a fleeting intermediate characterized by AA′BB′ pseudotriplets at δ −6.8 and 14.6 is seen (see inset of Figure 3) simultaneously with the onset of H_2 elimination, and the first appearance of $Pd_2X_2(\mu\text{-}S)(dmpm)_2$ (**2a**, δ_P −10.5). At −10 °C, only **1a** and **2a** are observed, and the disappearance of **1a** proceeds rapidly as the sample approaches ambient temperature.

The ^1H NMR spectra are also fully reversible from −90 to −40 °C (Figures 4 and 5). In the 1:1 **1a**/H_2S reaction at −80 °C, a singlet for dissolved H_2S is observed at δ 1.02 (0.04 ppm downfield from the H_2S signal in the absence of **1a**), and the diagnostic CH_2 signal of unreacted **1a** is seen at δ 2.66. The broad doublet at δ 2.02 (J_{HH} ∼ 15 Hz) and the broad signal at δ 3.42 are attributed to the CH_2 signals of **A**, the two signals implying an A-frame species. New dmpm-CH_3 signals are seen at δ 1.50−1.70, as well as two hydride signals in a 1:5 ratio at δ −9.80 and −9.97 that show no J_{PH} or J_{HH} coupling (Figure 5); these are assigned to **B** and **A**, respectively. Of note, the shifts of the major "hydride" signal and one of the CH_2 signals are temperature-dependent (see Figure 5, inset). In addition, a triplet at δ −0.81 (J_{PH} = 13.5 Hz) is resolved at −90 °C, and is assigned to the Pd−*SH* proton of **B**. However, this signal broadens and disappears at higher temperatures, presumably because of exchange of the *SH* proton with free H_2S. At −30 °C or above,

dx.doi.org/10.1021/ic200503d |*Inorg. Chem.* 2011, 50, 8094–8105

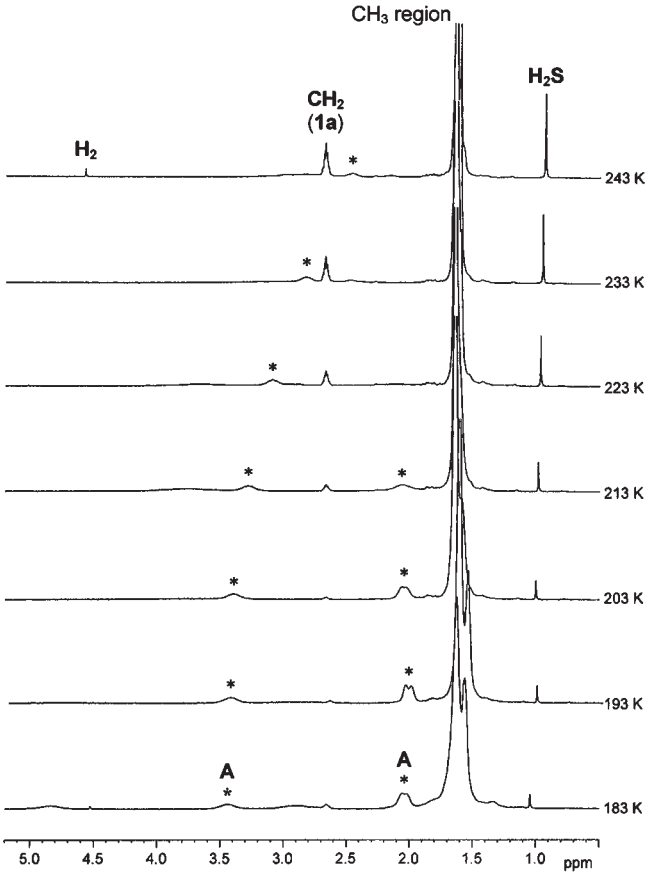

Figure 4. Variable temperature ^{1}H NMR spectra (300.1 MHz, CD_2Cl_2) on addition of H_2S (1.0 equiv) to $Pd_2Cl_2(dmpm)_2$ (**1a**) at lower temperatures. The methylene resonance(s) of **A** are labeled with asterisks.

irreversible H_2 evolution (seen at δ 4.58) and coformation of **2a** become evident. Proton resonances for the coordinated H_2S of the structurally characterized *cis*-$RuX_2(P{-}N)(PPh_3)(SH_2)$ in CD_2Cl_2 at −50 °C are seen at δ 0.30 and 1.49 (X = Cl), and at δ 0.48 and 1.23 (X = Br), while at 20 °C the signals collapse to a broad peak at δ ~1.0,[26] close to the signal for free H_2S. In these Ru complexes (P−N = [*o*-(*N*,*N*-dimethylamino)phenyl]diphenylphosphine) only one of the protons is coupled to only one of two P-atoms (the result of a Karplus relationship), while both H-atoms are involved in H-bonding with the halide ligands, and there are short SH···phenyl distances that could give rise to ring-current effects. A 1971 paper reports a ^{1}H signal at δ ~2.0 for a transient $Pt(PPh_3)_2(SH_2)$ species in CD_3Cl at room temperature en route to the more stable *trans*-$Pt(H)(SH)(PPh_3)_2$, which gave respective signals at δ −1.5 and −9.0 for the mercapto and hydrido ligands.[28a] Related to this, the high-field ^{1}H NMR signals for the SH and H ligands of *trans*-$Pd(H)(SH)(PCy_3)_2$ (Cy = cyclohexyl) are doublets of triplets δ −1.69 ($^3J_{HH}$ = 3.0 and $^3J_{PH}$ = 8.5 Hz) and −10.36 ($^3J_{HH}$ = 3.0 and $^2J_{PH}$ = 2.8 Hz), respectively,[28b] remarkably close to the chemical shifts of **B**; furthermore, the hydride resonances of the $Pd(H)(p\text{-}SC_6H_4R)(PCy_3)_2$ complexes (R = H, Me, OMe) are broad singlets at δ −11.0.[29] A review of transition metal-"hydrosulfido" complexes has appeared.[30] There is no doubt that **B** is a hydrido(mercapto) species, and we thought hopefully that **A** (δ_H −9.97 at −90 °C) might be the elusive H_2S-adduct, since no associated *SH* resonance was observed. However, this ^{1}H signal is in the Pd-hydride region and not in the coordinated H_2S region reported thus far (δ_H ~0−2.0, but only for mononuclear systems, see above), which argues against detection of an H_2S intermediate. Within a dinuclear system (see plausible asymmetric, fluxional species such as **I**−**III**, where partial Pd−Pd bonding may also be present), the H-atoms will become more hydridic, and it is less clear where the δ_H signals may appear. [The well established existence of μ-SR_2 metal complexes[31] suggests that μ-SH_2 species are certainly plausible]. The temperature-dependence of the δ −9.97 resonance (Figure 5, inset b) is consistent with a hydride being involved in an H-bond interaction (see below); however, the probability of the interaction being with the S-atom as part of a coordinated-H_2S moiety is considered minimal because the resonance is definitively in the hydride region.

The observed ABCD $^{31}P\{^1H\}$ pattern could in principle be consistent with species such as **I** (or with H_2S bonded at one Pd), **II**, or **III**. Geometries **II** and **III** are reminiscent of that seen in the structurally characterized silyl complex $Pd_2(\mu\text{-}SiHPh_2)_2(PEt_3)_2$ (**IV**) in which the Pd···Si···H agostic interaction dominates,[32a] while a secondary phosphine ligand of $[Pd_2(PH^tBu_2)_2(\mu\text{-}P^tBu_2)(\mu\text{-}PH^tBu_2)]OTf$ exhibits a similar pseudobridging coordination mode (**V**).[32b] The "hydride" resonance of **IV** appears as a broad doublet at δ 2.71,[32a] while that of **V** appears as a doublet of doublets at δ −0.16 with J_{PH} coupling to only the μ-P-atoms;[32b] such resonance values are thus not supportive of **A** species being of type **II** or **III**.

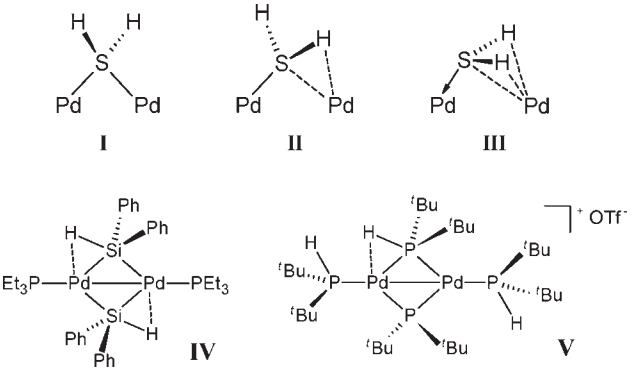

The single, relatively broad resonance observed in the hydride region for **A** throughout the accessible temperature range (Figure 5) suggests rapid exchange on the NMR-time scale of the H-atoms of the H_2S, likely of hydride and mercapto ligands. Several types of hydrido(mercapto) species, in which the H^- and SH^- ligands can be terminal or bridging (and which can migrate between the two positions) have been indentified during reactions of H_2S with $M_2(CO)_n(dppm)_2$ species that generate H_2 and a μ-sulfide product (M_2 = Ir_2, RuMo, RhMn, RhRe, and n = 3−6).[15] Bridging hydrides also exist in the bis(dialkylphosphino)methane complexes $[Ni_2X_2(\mu\text{-}R_2PCH_2PR_2)_2](\mu\text{-}H)$, where R = ^{i}Pr or cyclohexyl;[33a] Pd_2 complexes with chelated, nonbridged 1,3-bis(diisopropylphosphino)propane can also form semibridging hydride species,[33b] and the energy difference between terminal and bridging hydrides in related Pt systems has been shown to be small.[33c] Exchange within a coordinated H_2S species is also readily envisaged (Scheme 2).

The NMR data are consistent with a general mechanism of the type shown in Scheme 3; this is an extension of that suggested previously for the corresponding $Pd_2X_2(dppm)_2/H_2S$ systems (X = Br, I), where just one hydrido(mercapto) intermediate was detected.[12] An initially formed H_2S-adduct seems reasonable, but

dx.doi.org/10.1021/ic200503d |*Inorg. Chem.* 2011, 50, 8094–8105

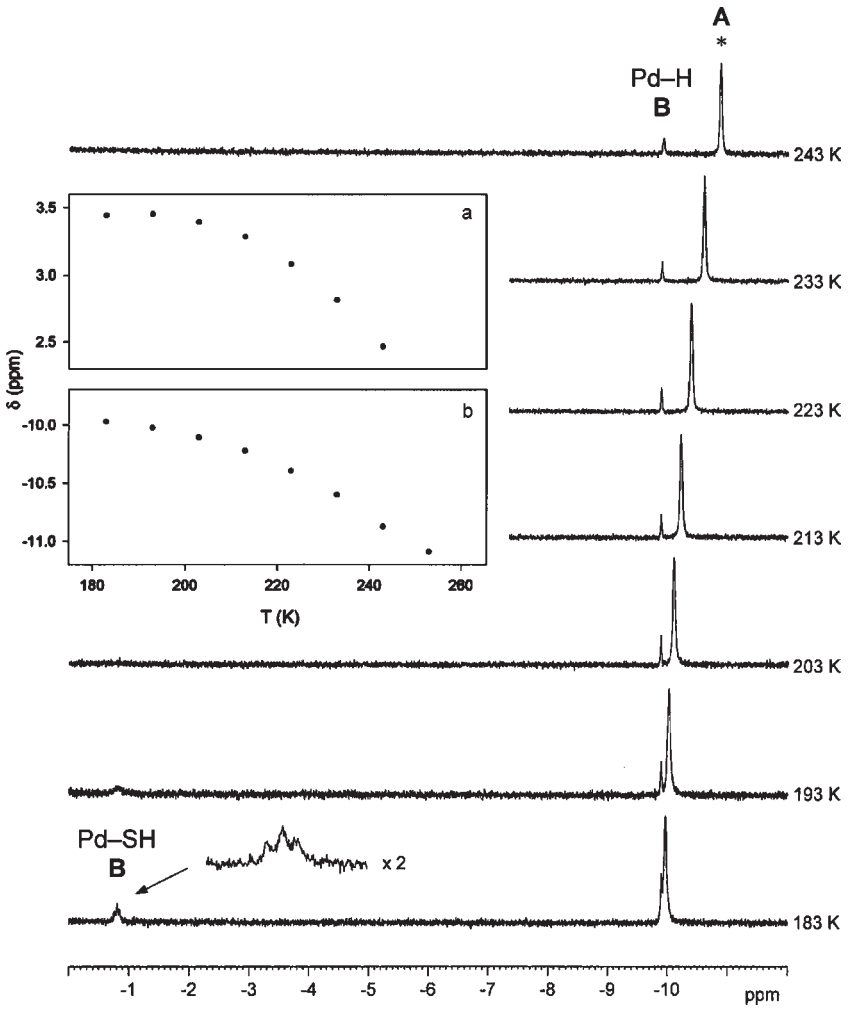

Figure 5. High-field VT ^{1}H NMR spectra (300.1 MHz, CD_2Cl_2) on addition of H_2S (1.0 equiv) to $Pd_2Cl_2(dmpm)_2$ (**1a**) at lower temperatures. Inset shows δ vs T plots for (a) one of the CH_2 signals (see also Figure 4); and (b) the signal assigned to the asterisk labeled **A**.

Scheme 2. Fluxionality of an H_2S Adduct

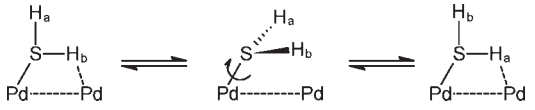

it is not impossible that H_2S can react in a concerted manner with a dimetallic precursor. In the dmpm system, **B** is plausibly the hydrido(mercapto) species illustrated, and **A** is likely some other hydrido(mercapto) species (see above) in rapid equilibrium with **B** (i.e., K_b is essentially a composite constant for two equilibria). Below −40 °C, **1a** is in equilibria with the stable **A** and **B**, and above this temperature H_2 elimination from **B** would yield the μ-sulfide derivative **2a**.

As the temperature is raised from −90 to −40 °C, the NMR signals of unreacted **1a** and free H_2S increase, implying that formation of the observed intermediates is exothermic, which is necessarily so since such chemistry is likely to be entropically unfavorable.[12] Accurate integration of the ^{1}H NMR signals was complicated by the unresolved and/or broad line-shapes, and determination of the free H_2S concentration was not possible because of the large temperature range used, this encompassing both the melting and the boiling points of the gas.

As noted above, the transitory $^{31}P\{^1H\}$ AA′BB′ pattern seen at −20 °C as pseudotriplets at δ −6.8 and 14.6 (apparent J_{PP} values of ∼35 Hz) coincides with the beginning of the H_2-elimination process. The pattern could be due to an unsymmetrical, deprotonated hydrido(mercapto) or η^2-H_2 species formed en route to H_2-elimination (see Scheme 3). Deprotonation of coordinated SH^- has been demonstrated in the reaction of H_2S at a Pt(111) surface, and in the reactions of $[M_3(\mu_3\text{-}CO)(dppm)_3][PF_6]_2$ (M = Pd, Pt) with H_2S, which afford $[M_3(\mu_3\text{-}S)(H)(dppm)_3]$-$PF_6$.[34] A related "reverse" intramolecular proton transfer from an η^2-H_2 ligand to the S-atom of an ancillary coligand is also well-known.[35]

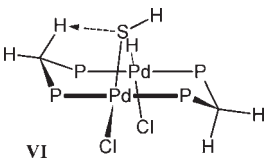

VI

The marked temperature-dependence of one of the CH_2 resonances of **A** could well result from an intramolecular interaction of a CH_2 proton with an SH ligand (as shown in **VI**). The behavior is reminiscent of that seen for amide protons of some

dx.doi.org/10.1021/ic200503d |*Inorg. Chem.* 2011, 50, 8094–8105

Scheme 3. Proposed Mechanism for the Reaction of 1a with H_2S

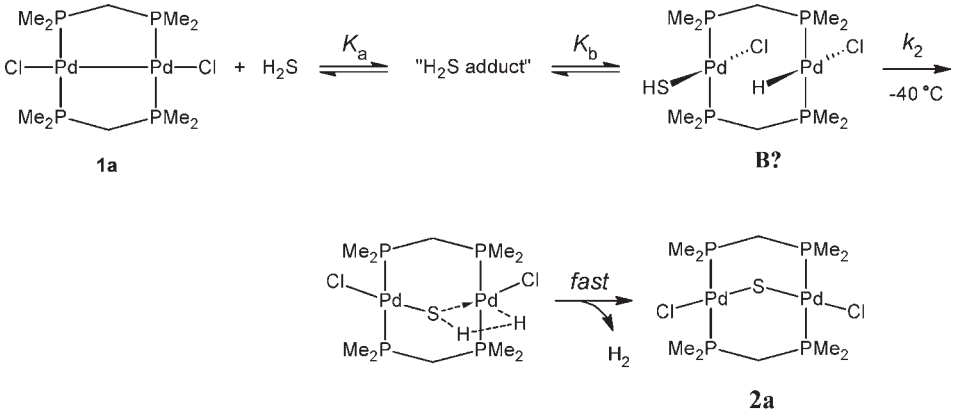

peptides, where increased thermal motion leads to a lengthening of H-bonds of the amide proton and typically upfield shifts as seen here (Figure 5); the amide protons are generally in rapid exchange on the NMR-time scale.[36] The CH_2 protons of dppm have been shown to act as H-bond donors via intramolecular (with CO ligands) or intermolecular interactions (with solvate molecules).[37]

The VT NMR data for the reaction of $Pd_2Cl_2(depm)_2$ (**1a′**) with H_2S to generate $Pd_2Cl_2(\mu\text{-}S)(depm)_2$ (**2a′**) are analogous to those of the **1a** → **2a** reaction, but there is evidence only for an **A′** species (analogous to **A**), where again no *SH* resonance is seen; no better defined hydrido(mercapto) such as **B** or transient, pseudotriplet AA′BB′ species was detected. The $^{31}P\{^1H\}$ and ^1H NMR spectra for the **1a′**/H_2S system in CD_2Cl_2, which can be reversibly cycled below −40 °C, are shown in the Supporting Information, Figures S1 and S2, respectively. In the $^{31}P\{^1H\}$ spectra at −80 °C, the singlet of **1a′** (δ −10.1) and two ABCD patterns are seen, centered at δ 13.5 and 20.3; the ABCD signals coalesce at about −40 °C and fade above this temperature with formation of **2a′** and H_2. The ABCD patterns at 213 K are analogous to the ABCD pattern observed at 193 K for the dmpm system (Figure.3), suggesting perhaps that the dmpm spectrum at 183 K is a composite one of two fluxional ABCD-type species. The larger depm ligand is expected to result in slower dynamic processes, better resolved low temperature spectra, and also less stable face-to-face intermediates such as **B** (Scheme 3). Above 0 °C in the depm system, only the singlets of **1a′** (δ −10.8) and **2a′** (δ 10.9) are seen, and the formation of **2a′** is essentially complete after 20 min at room temperature.

The $^{31}P\{^1H\}$ shifts of **A′** and **2a′** are ∼20 ppm downfield of those for the corresponding dmpm species, but this almost certainly results from a similar difference in the shifts for free dmpm and depm (−54.5 and −27.9 ppm in CD_3Cl at 20 °C, respectively); there is a similar difference in the $^{31}P\{^1H\}$ shifts of **1a′** and **1a**.[7,27] Although the chloro-and bromo-sulfido analogues **2a** (δ_P −10.5) and **2b** (δ_P −12.7) have chair and extended boat conformations, respectively, such differences in the solid state structures do not appear to be reflected in the solution NMR data. In the ^1H NMR spectrum at −80 °C, the H_2S signal at δ 1.00, and a series of broad multiplets at δ 1.54, 1.88, 2.58, 3.28, and 3.40 are generated; the δ 3.40 signal is resolved as a doublet (J_{HH} = 15.0 Hz) in the $^1H\{^{31}P\}$ NMR spectrum. At −40 °C, the

Scheme 4. Reaction of $Pd_2Cl_2(dmpm)_2$ (1a) with COS[a]

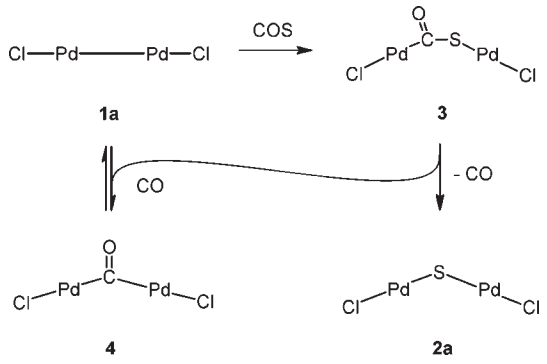

[a] μ-dmpm ligands omitted.

δ 3.40 signal, unlike the similar one seen in the **1a**/H_2S system, appears as a moderately well-resolved quintet (J_{PH} = 9.1 Hz). The high-field hydride resonance associated with **A′** (at −80 °C) is seen as a broad signal at δ −9.84, essentially the same as that assigned to **A** in the dmpm system (Figure 5), and the nature of the fluxional **A′** species is also certainly the same as for **A**. The hydride and methylene δ 3.40 shifts are again temperature-dependent.

Reactions of $Pd_2Cl_2(dmpm)_2$ (1a) and $Pd_2Cl_2(depm)_2$ (1a′) with COS. When COS is bubbled through a CH_2Cl_2 solution of **1a** at room temperature, the color rapidly turns red, and addition of hexanes after 4 h selectively precipitates pure **2a**, the bridged-sulfide complex. There is no reaction of **1a** with COS at −78 °C, but the system (Scheme 4) is conveniently monitored at −20 °C by $^{31}P\{^1H\}$ NMR spectroscopy (Figure 6). After 20 min, the singlets of **1a**, **2a** and the known $Pd_2Cl_2(\mu\text{-}CO)(dmpm)_2$ (**4**)[13,18] are seen, as well as an AA′BB′ pattern (two pseudotriplets at δ −3.5 and −13.4, apparent J_{PP} ∼18 Hz) that is attributed to $Pd_2Cl_2(\mu\text{-}COS)(dmpm)_2$ (**3**). The triplets are essentially the same as those seen for the known $Pd_2Cl_2(\mu\text{-}CS_2)(dmpm)_2$ complex (**5**),[18] which is formed from the room temperature reaction of **1a** with excess CS_2; the proposed structure of **5** (and substantiated here by an X-ray structure, see below) is one containing an unsymmetrical $\mu\text{-}\eta^2\text{-}C,S$ bound CS_2.[18] Species **3** is thus assumed to have an analogously bound COS. The μ-CO complex **4** could be formed via reaction of **1a**

dx.doi.org/10.1021/ic200503d |*Inorg. Chem.* 2011, 50, 8094–8105

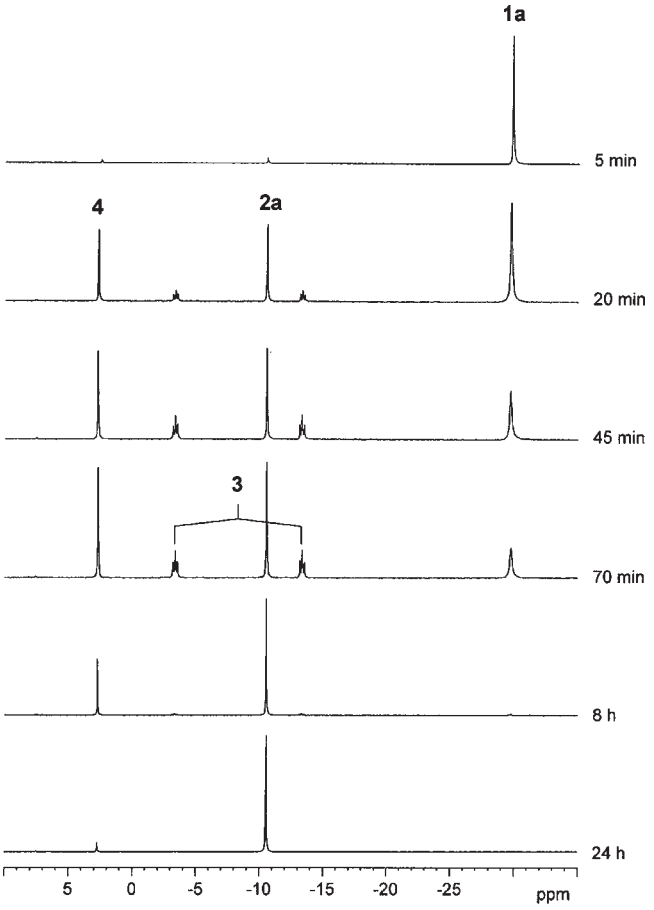

Figure 6. $^{31}P\{^{1}H\}$ NMR spectra (121.5 MHz, CD_2Cl_2) recorded during reaction of $Pd_2Cl_2(dmpm)_2$ (**1a**) with COS (1 atm). After 70 min at −20 °C, the sample was warmed to 20 °C, and spectra acquired after 8 and 24 h were measured at this temperature.

with CO derived from the decarbonylation of **3** (as shown in Scheme 4), although insertion of elemental sulfur into a metal-CO bond has been demonstrated in the synthesis of the structurally characterized $(\eta^5\text{-MeCp})_2Nb(\eta^2\text{-COS})CH_2SiMe_2$ (where COS acts as a η^2-*C,S* ligand)[38] and so a step involving the reverse, a direct loss of "S" from the coordinated COS of **3** to form **4**, remains a possibility. After 8 h, no **1a** or **3** is present, and subsequently the amount of **4** gradually decreases because the CO-binding to **1a** is reversible[18] and presumably the CO would eventually diffuse into the gas phase inside the NMR-tube; **2a** accumulates as the thermodynamic product. Attempts to isolate **3** were unsuccessful but, after ∼1 h at −20 °C, there was a sufficient amount to allow for its further in situ characterization by ^1H NMR spectroscopy (Figure 7a), where two doublets of quintets are attributed to the dmpm-CH_2 protons.

The X-ray structure of $Pd_2Cl_2(\mu\text{-}CS_2)(dmpm)_2$ (**5**) is shown in Figure 8, and selected metrical parameters are given in Tables 1−3. The asymmetric unit contains disordered CH_2Cl_2 and Et_2O solvent molecules that are not discussed; elemental analysis and ^1H NMR data (Figure 7b) are consistent with the presence of ∼0.3 mol of each solvent. The structure closely resembles that of the $Pt_2Cl_2(\mu\text{-}CS_2)(dppm)_2$;[39a] the PdPt analogue has been reported, but only as an in situ species.[39b] Specifically, the $Pd_2P_4C_2$ ring in **5** adopts a distorted boat conformation with severe twisting about the P−Pd−P axes, and as a result the η^2-CS_2 ligand bridges a Pd···Pd distance of 3.088 Å, significantly shorter than in **2a** (3.342 Å) which has a chair conformation. The Pd−Cl bond lengths are consistent with calculations suggesting that the C-atom of a bridging CS_2 ligand exerts a stronger trans influence than does the S-atom.[40] The C−S bond lengths (1.708 and 1.651 Å) are longer than those found in gas-phase CS_2 (C−S = 1.56 Å).[41] The solid-state structure of **5** and the solution NMR spectroscopic data for **3** and **5** provide convincing evidence for the proposed formulation of **3** in solution. Attempts to desolvate a sample crystalline **5** at 78 °C in vacuo generated a mixture of **5**, **1a**, and **2a** (presumably via loss of CS from **5**), as determined by solution $^{31}P\{^{1}H\}$ NMR analysis of the residual solid. No evidence was seen for a CS adduct such as $Pd_2Cl_2(\mu\text{-CS})(dmpm)_2$ when a $CDCl_3$ solution of **5** was refluxed.

There was no NMR evidence for formation of an η^2-COS adduct with $Pd_2Cl_2(depm)_2$ (**1a′**) at −20 °C in CD_2Cl_2, although warming up to 20 °C slowly generated $Pd_2Cl_2(\mu\text{-CO})(depm)_2$ and $Pd_2Cl_2(\mu\text{-S})(depm)_2$ (**2a′**); after 48 h, the latter was present in >90% yield, presumably via decarbonylation of a transient COS intermediate. Treatment of **1a′** with CS_2 gives quantitatively $Pd_2Cl_2(\mu\text{-}CS_2)(depm)_2$ (**5′**) that was characterized in situ by NMR in CD_2Cl_2, although the PCH_2P methylene resonances were obscured by overlapping CH_2 resonances of the depm ligand. The AA′BB′ pseudo-triplets pattern seen in the $^{31}P\{^{1}H\}$ NMR is consistent with a structure analogous to that of **5**. Attempts to isolate **5′** yielded a mixture containing **1a′**, implying loss of CS_2 during the workup procedure.

The $Pd_2Cl_2(dppm)_2$ complex in CD_2Cl_2 was found to be unreactive toward COS or CS_2, presumably because the phenyl groups sterically prevent formation of the distorted boat configuration needed to accommodate a bridged heterocumulene ligand.

A review on metal complexes of COS, CS_2, and CO_2[41] reveals that the coordination chemistry of COS is more limited than that of CS_2, with COS complexes being usually prepared from reaction of a coordinatively unsaturated metal species with COS. Unstable species of the type $Pd(COS)(EPh_3)_2$ (E = P, As, Sb) are known,[42] while $Pd[SC(O)dmpz]_2$ is formed via COS insertion into a Pd−N bond of $[Pd(dmpz)_2(Hdmpz)]_2$ (Hdmpz = 3,5-dimethylpyrazole).[43] There are examples of COS acting as a μ-η^2-*C,S* ligand (e.g., in $[RhCl(COS)(SbPh_3)]_2$[44]), but **3** appears to be the only known example of a detected $Pd_2(\mu\text{-COS})$ species. Reaction of $[Pd(H)(PMe_3)_3]BPh_4$ with COS gives $[Pd_3(\mu\text{-S})(PMe_3)_6][BPh_4]_2$ containing a triply bridging sulfide ligand.[45] In a related process also involving loss of CO, reaction of $Pt_2(\mu\text{-dppm})_3$ with COS generates $Pt_2(\mu\text{-S})(\mu\text{-dppm})(\eta^1\text{-dppm})_2$ via a supposed $Pt_2(\mu\text{-COS})$ intermediate;[46] the analogous COS reaction with $Pd_2(\mu\text{-dppm})_3$ has not been reported.

CONCLUSIONS

Reactions of $Pd_2X_2(\mu\text{-}R_2PCH_2PR_2)_2$ complexes (X = halogen, R = Me or Et) in CH_2Cl_2 solution with H_2S, S_8, COS, and CS_2 are presented, and notable differences are seen compared to corresponding reactions of the analogous R = Ph complexes, although bridged Pd−S−Pd species appear to be the favored thermodynamic product in all the systems. The H_2S systems liberate H_2 as coproduct and, at low temperature in the dmpm amd depm systems, hydrido(mercapto) intermediates are seen;

dx.doi.org/10.1021/ic200503d |*Inorg. Chem.* 2011, 50, 8094–8105

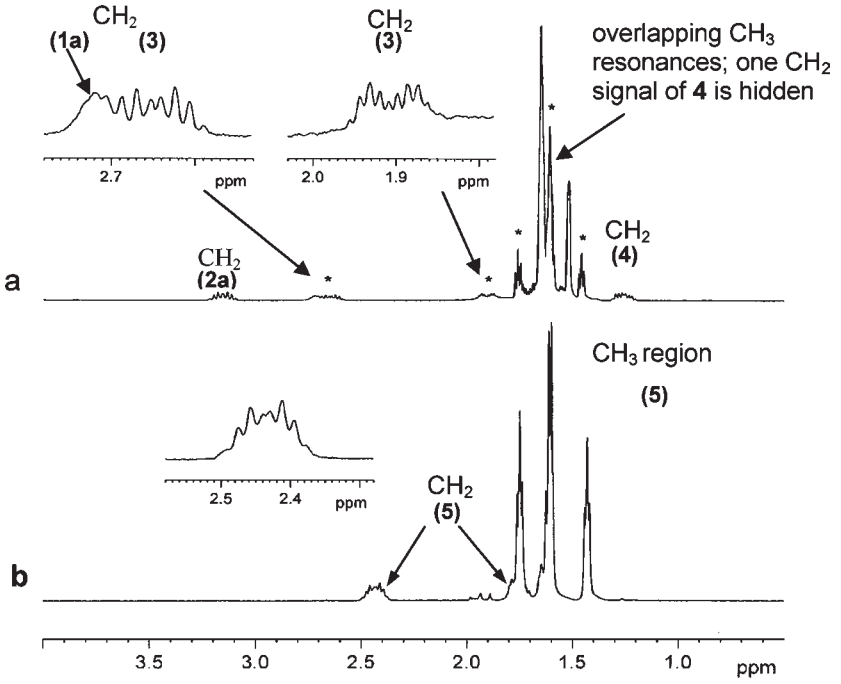

Figure 7. ^{1}H NMR spectra (300.1 MHz, CD_2Cl_2, after −20 °C) of: (a) the mixture formed on reaction of $Pd_2Cl_2(dmpm)_2$ (**1a**) with 1 atm of COS after 1 h; and (b) pure $Pd_2Cl_2(\mu\text{-}CS_2)(dmpm)_2$ (**5**). Signals in (a) assigned to $Pd_2Cl_2(\mu\text{-}COS)(dmpm)_2$ (**3**) are labeled with an asterisk; the insets show expansions of the CH_2 signals of **3** and **5**.

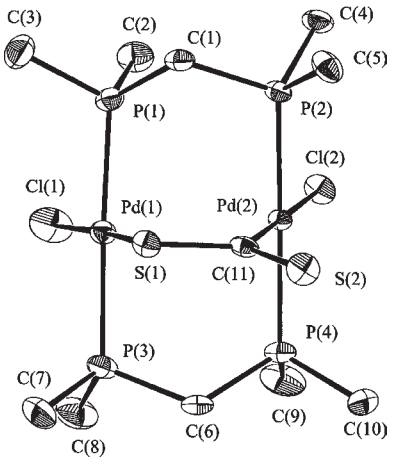

Figure 8. ORTEP diagram of $Pd_2Cl_2(\mu\text{-}CS_2)(dmpm)_2$ (**5**) with thermal ellipsoids shown at the 50% probability level.

H_2S-adducts are not definitively identified. Only the dialkyl species and not the dppm complex react with COS and CS_2. In the COS systems, an intermediate μ-η^2-*C,S* bound COS species is seen in the R = Me system, while μ-CO intermediates are seen in both dialkyl systems. The CS_2 reactions form products containing μ-η^2-*C,S* bound CS_2; these are thermally unstable, but the X-ray structure of the known R = Me complex was determined. The precursor X = Cl complexes are the most reactive, likely because of steric problems resulting from the larger halogen ligands that prevent configurational changes needed to accommodate the geometry of reaction intermediates; similarly, the more hindered R = Ph reactants are unreactive toward COS and CS_2.

EXPERIMENTAL SECTION

General Procedures. Unless otherwise noted, all synthetic procedures were carried out using standard Schlenk techniques under dry N_2 at room temperature (~20 °C). Reagent grade solvents were distilled under N_2 from the appropriate standard drying agent. Deuterated solvents were obtained from Cambridge Isotope Laboratories and were used as received. H_2S (Matheson) and COS (Aldrich) were obtained from commercial sources and were used without further purification. D_2S was prepared from the reaction of DCl (Aldrich, 37 wt % solution in D_2O, 99 atom % D) with CaS (Fisher) ; the evolved gas was bubbled through D_2O and dried over P_2O_5. Reactions with the odoriferous and toxic gases were carried out in a well-ventilated fumehood; for preparative reactions, a stream of the gas was bubbled through a solution of a complex, and the reaction mixture was then sealed under 1 atm of the gas. Gas-tight Sample-Lok syringes (Dynatech) were also used for handling gaseous reagents; after a syringe was flushed with the gas, a known quantity (at ambient conditions) was injected into a septum-sealed reaction vessel or NMR tube.

The complexes $Pd_2X_2(dmpm)_2$ (X = Cl (**1a**),[47] Br (**1b**),[27] I (**1c**),[7] the depm analogues (**1a′**, **1b′**, **1c′**, and **1d′**),[7] $Pd_2Cl_2(\mu\text{-}CO)(dmpm)_2$,[13,18] $Pd_2Cl_2(\mu\text{-}CS_2)(dmpm)_2$ (**5**),[13,18] $Pd_2Cl_2(dppm)_2$[48] and $Pd_2I_2(\mu\text{-}S)(dppm)_2$,[3d] were prepared by the reported methods.

NMR spectra were recorded on a Bruker AV300 spectrometer (300.13 MHz for ^{1}H, 121.49 MHz for ^{31}P). Residual deuterated solvent proton (relative to external $SiMe_4$) or external $P(OMe)_3$ (^{31}P, δ 141.0 relative to 85% aq H_3PO_4) was used as a reference (s = singlet, d = doublet, t = triplet, q = quartet, qn = quintet, m = multiplet, br = broad). *J* values are reported in hertz (Hz). Stoichiometric reactions of **1a** and **1a′** with H_2S were monitored at low temperature by injecting H_2S into a septum-sealed NMR tube containing a cold (−80 °C) CD_2Cl_2 solution of the complex. The NMR tube was shaken and placed in the cooled probe of the spectrometer, and left for ~10 min for the system to equilibrate; spectra were then recorded at −80 °C and then in 10° increments up to 20 °C, the reversibility of a spectral change being demonstrated by repeatedly

dx.doi.org/10.1021/ic200503d |*Inorg. Chem.* 2011, 50, 8094–8105

cycling the temperature. UV−vis absorption spectra were recorded on a Hewlett-Packard 8452A diode-array spectrometer, data being presented as λ_{max} in nm ($\varepsilon_{max} \times 10^{-3}$, M^{-1} cm^{-1}). Elemental analyses were performed by Mr. P. Borda of the Microanalytical Service in this department.

X-ray Crystallographic Analyses. The structures are shown in Figures 1, 2, and 8. Some crystallographic data are given in Table 1, and selected bond lengths and angles are given in Tables 2 and 3. Full crystallographic data are given in the Supporting Information. Crystalline samples of **2a**, **2b** and solvated **5** were prepared by layering CH_2Cl_2 solutions of the complexes with Et_2O. X-ray analyses were carried out at 180 K on a Rigaku/ADSC CCD area detector with graphite monochromated MoKα radiation (0.71069 Å). The final unit-cell parameters were based on 15382 reflections with $2\theta_{max}$ = 60.1° for **2a**, 8377 reflections with $2\theta_{max}$ = 60.0° for **2b**, and 26060 reflections with $2\theta_{max}$ = 60.1° for the solvated **5**, in a series of ϕ and ω scans in 0.50° oscillations with respective exposures of 15−20 s; the crystal-to-detector distance was ∼39 mm. Data were processed using the d*TREK area detector program,[49] and the structures were solved by direct methods.[50] All refinements were performed using the SHELXL-97 program[51] via the WinGX interface.[52]

All non-H-atoms in the three structures were refined anisotropically. All the H-atoms were fixed in idealized, calculated positions. The asymmetric unit of **5** contains disordered solvate molecules (CH_2Cl_2 and/or Et_2O); however, given the nature of the overlap of disordered fragments, it was not possible to obtain a reasonable model. As a result, the PLATON/SQUEEZE[53] program was used to generate a "solvent free" data set.

Preparation of $Pd_2Cl_2(\mu$-S)(dmpm)$_2$ (2a). *Method 1.* H_2S (1 atm) was added to a solution of **1a** (147 mg, 0.265 mmol) in CH_2Cl_2 (20 mL), and the resulting red solution was stirred for 1 h. The solution was evaporated to ∼8 mL, and hexanes (20 mL) were added to precipitate an orange solid that was isolated by filtration, washed with Et_2O (2 × 10 mL), and dried in vacuo at 78 °C. Yield: 144 mg (93%). ^{1}H NMR (CD_2Cl_2): δ 1.60 (br m, 12H, CH_3), 1.65 (br m, 12H, CH_3), 1.71 (dqn, 2H, CH_2, J_{PH} = 3.4, $^2J_{HH}$ = 13.7), 3.15 (dqn, 2H, CH_2, J_{PH} = 5.8, $^2J_{HH}$ = 13.5). ^{1}H{^{31}P} NMR (CD_2Cl_2): δ 1.60 (s, 12H, CH_3), 1.65 (s, 12H, CH_3), 1.71 (d, 2H, CH_2, $^2J_{HH}$ = 13.7), 3.15 (d, 2H, CH_2, $^2J_{HH}$ = 13.5). ^{31}P{^{1}H} NMR (CD_2Cl_2): δ −10.5 (s). UV−vis (CH_2Cl_2): 270 (18.6), 302 sh (10.8), 460 (0.70). Anal. Calcd for $C_{10}H_{28}Cl_2P_4Pd_2S$: C, 20.43; H, 4.80; S, 5.45. Found: C, 20.61; H, 4.74; S, 5.53.

Method 2. COS was bubbled through a solution of **1a** (50 mg, 0.091 mmol) in CH_2Cl_2 (6 mL) for 15 min, and then the solution was stirred under COS (1 atm) for 4 h. The workup procedure described above yielded 48 mg of **2a** (90%).

Method 3. Elemental S_8 (0.90 mg, 0.028 mmol, 1 mol equiv S) was added to a solution of **1a** (15 mg, 0.027 mmol) in $CDCl_3$. The cloudy red mixture was shaken for 20 min prior to NMR analysis, which indicated >95% conversion to **2a**; use of excess sulfur results in decomposition of **2a** and formation of dmpm(S)$_2$, the only P-containing product (δ_P 32.5 in $CDCl_3$).[11]

Preparation of $Pd_2Br_2(\mu$-S)(dmpm)$_2$ (2b). H_2S was bubbled through a solution of **1b** (55 mg, 0.085 mmol) in CH_2Cl_2 (10 mL) for 5 min, and the resulting red solution was stirred under H_2S (1 atm) for 1 h. The solution was evaporated to ∼4 mL prior to addition of hexanes (10 mL), which initiated the formation of a red precipitate that was collected, washed with Et_2O (2 × 5 mL), and dried in vacuo at 78 °C. Yield: 51 mg (92%). ^{1}H NMR (CD_2Cl_2): δ 1.66 (dqn, 2H, CH_2, J_{PH} = 3.3, $^2J_{HH}$ = 13.4), 1.70 (m, 12H, CH_3), 1.75 (m, 12H, CH_3), 3.31 (dqn, 2H, CH_2, J_{PH} = 5.9, $^2J_{HH}$ = 13.3). ^{1}H{^{31}P} NMR (CD_2Cl_2): δ 1.66 (d, 2H, CH_2, $^2J_{HH}$ = 13.4), 1.70 (s, 12H, CH_3), 1.75 (s, 12H, CH_3), 3.31 (d, 2H, CH_2, $^2J_{HH}$ = 13.3). ^{31}P{^{1}H} NMR (CD_2Cl_2): δ −12.7 (s). UV−vis (CH_2Cl_2): 278 (24.7), 324 (13.7), 462 (3.20). Anal. Calcd for $C_{10}H_{28}Br_2P_4Pd_2S$: C, 17.74; H, 4.17; S, 4.74. Found: C, 18.00; H, 4.00; S, 4.78.

Preparation of $Pd_2I_2(\mu$-S)(dmpm)$_2$ (2c). *Method 1.* To a solution of $Pd_2I_2(\mu$-S)(dppm)$_2$ (126 mg, 0.099 mmol) in CH_2Cl_2 was added dmpm (29 mg, 0.215 mmol). The resulting orange solution was stirred for 2 h, and then the solution was evaporated to ∼5 mL. The slow addition of hexanes (15 mL) initiated formation of an orange-brown precipitate that was isolated by filtration, washing with hexanes (2 × 5 mL), and drying in vacuo at 78 °C. Yield: 64 mg (94%). ^{1}H NMR (CD_2Cl_2): δ 1.73 (m, 12H, CH_3), 1.85 (m, 12H, CH_3), 3.55 (dqn, 2H, CH_2, J_{PH} = 6.1, $^2J_{HH}$ = 13.2. A second CH_2 dqn is obscured by the CH_3 signal at δ 1.73. ^{1}H{^{31}P} NMR (CD_2Cl_2): δ 1.73 (s, 12H, CH_3), 1.85 (s, 12H, CH_3), 3.55 (d, 2H, CH_2, $^2J_{HH}$ = 13.2). A second CH_2 doublet is partially visible behind the CH_3 signal at δ 1.73. ^{31}P{^{1}H} NMR (CD_2Cl_2): δ −16.1 (s). UV−vis (CH_2Cl_2): 290 (20.7), 354 (7.70). Anal. Calcd for $C_{10}H_{28}I_2P_4Pd_2S$: C, 15.58; H, 3.66; S, 4.16. Found: C, 15.91; H, 3.64; S, 4.33.

Method 2. H_2S (1 atm) was added to a septum-sealed NMR tube containing a solution of **1c** (10 mg, 0.014 mmol) in CD_2Cl_2, and the tube was shaken vigorously prior to analysis by ^{31}P{^{1}H} NMR spectroscopy. Conversion to **2c** and H_2 was essentially complete after 8 h.

Preparation of $Pd_2Cl_2(\mu$-S)(depm)$_2$ (2a′). *Method 1.* H_2S was bubbled through a solution of Pd_2Cl_2(depm)$_2$ (**1a′**) (77 mg, 0.115 mmol) in CH_2Cl_2 (10 mL) for 5 min, and the solution was stirred under H_2S (1 atm) for 1 h. The solution was filtered through Celite, and the filtrate was evaporated to ∼3 mL, when a red precipitate was formed on the addition of hexanes (20 mL). The solid was filtered off, washed with hexanes (10 mL) and dried in vacuo. Yield: 71 mg (89%). ^{1}H NMR (CD_2Cl_2): δ 1.20 (m, 24H, CH_3), 1.72 (dqn, 2H, PCH_2P, J_{PH} = 3.2, $^2J_{HH}$ = 13.7), 1.91 (br m, 4H, CH_2CH_3), 2.02 (br m, 8H, CH_2CH_3), 2.31 (br m, 4H, CH_2CH_3), 2.87 (dqn, 2H, PCH_2P, J_{PH} = 5.8, $^2J_{HH}$ = 13.7). ^{1}H{^{31}P} NMR (CD_2Cl_2): δ 1.18 (t, 12H, CH_3, $^3J_{HH}$ = 7.6), 1.22 (t, 12H, CH_3, $^3J_{HH}$ = 7.6), 1.72 (d, 2H, PCH_2P, $^2J_{HH}$ = 13.7), 1.91 (dq, 4H, CH_2CH_3, $^2J_{HH}$ = 15.5, $^3J_{HH}$ = 7.6), 2.02 (dq, 8H, $^3J_{HH}$ = 7.6, $^2J_{HH}$ is unresolved), 2.31 (dq, 4H, CH_2CH_3, $^2J_{HH}$ = 15.5, $^3J_{HH}$ = 7.6), 2.87 (d, 2H, PCH_2P, $^2J_{HH}$ = 13.7). ^{31}P{^{1}H} NMR ($CDCl_3$): δ 9.2 (s). UV−vis ($CHCl_3$): 250 (20.5), 272 (20.8), 308 (12.0), 466 (1.20). Anal. Calcd for $C_{18}H_{44}Cl_2P_4Pd_2S$: C, 30.88; H, 6.33; S, 4.58. Found: C, 30.89; H, 6.36; S, 4.81.

Method 2. To a solution of **1a′** (11 mg, 0.016 mmol) in CD_2Cl_2 was added elemental S_8 (4.2 mg, 0.131 mmol, 8.0 mol equiv. S). When the mixture was shaken, the solution color rapidly changed from orange to red. Analysis by ^{31}P{^{1}H} NMR spectroscopy after 15 min indicated quantitative conversion to **2a′**.

Preparation of $Pd_2X_2(\mu$-S)(depm)$_2$ [X = Br (2b′), I (2c′)]. A solution of **2a′** (49 mg, 0.070 mmol) in CH_2Cl_2 (10 mL) was treated with a solution of NaBr (69 mg, 0.676 mmol) in MeOH (5 mL). The orange solution was stirred at room temperature for 2.5 h and then evaporated to dryness. The residue was extracted with CH_2Cl_2 (4 × 5 mL), the mixture filtered through Celite, and the volume reduced to ∼5 mL in vacuo. The orange solid that precipitated on addition of hexanes (10 mL) was collected, and dried at 100 °C in vacuo. Yield: 40 mg (73%). ^{1}H NMR ($CDCl_3$): δ 1.18 (m, 24H, CH_3), 1.75 (dqn, 2H, PCH_2P, J_{PH} = 3.1, $^2J_{HH}$ = 13.7), 1.94 (br m, 4H, CH_2CH_3), 2.07 (br m, 8H, CH_2CH_3), 2.42 (br m, 4H, CH_2CH_3), 2.98 (dqn, 2H, PCH_2P, J_{PH} = 5.8, $^2J_{HH}$ = 13.7). ^{1}H{^{31}P} NMR (CD_2Cl_2): δ 1.17 (t, 12H, CH_3, $^3J_{HH}$ = 7.7), 1.20 (t, 12H, CH_3, $^3J_{HH}$ = 7.7), 1.75 (d, 2H, PCH_2P, $^2J_{HH}$ = 13.7), 1.94 (dq, 4H, CH_2CH_3, $^2J_{HH}$ = 15.6, $^3J_{HH}$ = 7.7), 2.07 (q, 8H, $^3J_{HH}$ = 7.7), 2.42 (dq, 4H, CH_2CH_3, $^2J_{HH}$ = 15.5, $^3J_{HH}$ = 7.6), 2.98 (d, 2H, PCH_2P, $^2J_{HH}$ = 13.7). ^{31}P{^{1}H} NMR ($CDCl_3$): δ 9.5 (s). Anal. Calcd for $C_{18}H_{44}Br_2P_4Pd_2S$: C, 27.40; H, 5.62; S, 4.06. Found: C, 27.68; H, 5.69; S, 4.22.

Similarly, a solution of **2a′** (30 mg, 0.043 mmol) in CH_2Cl_2 (10 mL) reacts with a solution of NaI (130 mg, 0.867 mmol) in MeOH (5 mL) to yield **2c′**. Yield: 28 mg (74%). ^{1}H NMR ($CDCl_3$): δ 1.20 (m, 24H, CH_3), 1.88 (dqn, 2H, PCH_2P, J_{PH} = 3.0, $^2J_{HH}$ = 13.5), 2.02 (br m, 4H, CH_2CH_3), 2.20 (br m, 8H, CH_2CH_3), 2.61 (br m, 4H, CH_2CH_3), 3.23

dx.doi.org/10.1021/ic200503d |Inorg. Chem. 2011, 50, 8094–8105

(dqn, 2H, PCH_2P, J_{PH} = 6.3, $^2J_{HH}$ = 13.5). $^1H\{^{31}P\}$ NMR (CD_2Cl_2): 1.19 (t, 12H, CH_3, $^3J_{HH}$ = 7.6), 1.21 (t, 12H, CH_3, $^3J_{HH}$ = 7.6), 1.88 (d, 2H, PCH_2P, $^2J_{HH}$ = 13.5), 2.02 (dq, 4H, CH_2CH_3, $^2J_{HH}$ = 15.6, $^3J_{HH}$ = 7.7), 2.20 (dq, 8H, $^3J_{HH}$ = 7.7, $^2J_{HH}$ is unresolved), 2.61 (dq, 4H, CH_2CH_3, $^2J_{HH}$ = 15.6, $^3J_{HH}$ = 7.6), 3.23 (d, 2H, PCH_2P, $^2J_{HH}$ = 13.5). $^{31}P\{^1H\}$ NMR ($CDCl_3$): δ 7.9 (s). Anal. Calcd for $C_{18}H_{44}I_2P_4Pd_2S$: C, 24.48; H, 5.02; S, 3.63. Found: C, 24.64; H, 5.04; S, 3.79.

In Situ Reaction of $Pd_2Cl_2(dmpm)_2$ (1a) with COS. To a septum-sealed NMR tube containing **1a** (10 mg, 0.018 mmol) in CD_2Cl_2 at −78 °C was added COS (1 atm); the yellow solution rapidly turned red. The ^1H, $^1H\{^{31}P\}$, and $^{31}P\{^1H\}$ NMR spectra of the solution were recorded periodically as the NMR tube was warmed to room temperature (see Figures 6 and 7). Characterization data for $Pd_2Cl_2(\mu\text{-COS})(dmpm)_2$ (**3**): ^1H NMR (CD_2Cl_2, 20 °C): δ 1.46 (t, 6H, CH_3, J_{PH} = 3.4), ∼1.6 (br, 12H, CH_3), 1.76 (t, 6H, CH_3, J_{PH} = 3.9), 1.91 (dqn, 2H, CH_2, J_{PH} = 3.7, $^2J_{HH}$ = 14.4), 2.65 (dqn, 2H, CH_2, J_{PH} = 5.2, $^2J_{HH}$ = 14.4). $^1H\{^{31}P\}$ NMR (CD_2Cl_2, 20 °C): δ 1.46 (s, 6H, CH_3), 1.60 (s, 6H, CH_3), 1.62 (s, 6H, CH_3 of **3**), 1.76 (s, 6H, CH_3), 1.91 (d, 2H, CH_2, $^2J_{HH}$ = 14.4), 2.65 (d, 2H, CH_2, $^2J_{HH}$ = 14.4). $^{31}P\{^1H\}$ NMR (CD_2Cl_2, 20 °C): δ −3.5 and −13.4 (AA′BB′). Characterization data for $Pd_2Cl_2(\mu\text{-CO})(dmpm)_2$ (**4**): ^1H NMR (CD_2Cl_2, 20 °C): δ 1.26 (dqn, 2H, CH_2, J_{PH} = 4.5, $^2J_{HH}$ = 14.1), 1.52 (br s, 12H, CH_3), 1.57 (dqn, 2H, CH_2, J_{PH} = 2.7, $^2J_{HH}$ = 14.1), 1.65 (br s, 12H, CH_3). $^1H\{^{31}P\}$ NMR (CD_2Cl_2, 20 °C): δ 1.26 (d, 2H, CH_2, $^2J_{HH}$ = 14.1), 1.52 (s, 12H, CH_3), 1.57 (d, 2H, CH_2, $^2J_{HH}$ = 14.1), 1.65 (s, 12H, CH_3). $^{31}P\{^1H\}$ NMR (CD_2Cl_2, 20 °C): δ 2.6 (s). These spectral data are identical to those of a sample of **4** isolated from the reaction of **1a** with CO:[13,18] Anal. Calcd for $C_{11}H_{28}Cl_2OP_4Pd_2$: C, 22.63; H, 4.83. Found: C, 22.63; H, 4.87.

Preparation of $Pd_2Cl_2(\mu\text{-}CS_2)(dmpm)_2$ (5). Complex **5** was prepared according to a published procedure.[18] To a solution of $Pd_2Cl_2(dmpm)_2$ (**1a**) (10 mg, 0.018 mmol) in CH_2Cl_2 (2 mL) in an NMR tube was added CS_2 (0.050 mL, 63 mg, 0.829 mmol). The resulting orange-red solution was layered with Et_2O (1 mL), and red crystals were collected from the walls of the NMR tube after 72 h. Elemental analysis and X-ray crystallographic data confirmed the presence of CH_2Cl_2 and Et_2O solvate molecules; attempts to dry the isolated crystals in vacuo at room temperature resulted in the loss of CS_2. Attempts to precipitate **5** by adding Et_2O or hexanes to a concentrated CH_2Cl_2 solution of **5** gave mixtures of **1a** and **5**, as determined by $^{31}P\{^1H\}$ NMR spectroscopy. ^1H NMR (CD_2Cl_2): δ 1.43 (t, 6H, CH_3, J_{PH} = 3.4), 1.60 (t, 6H, CH_3, J_{PH} = 4.1), 1.62 (t, 6H, CH_3, J_{PH} = 4.1), 1.75 (t, 6H, CH_3, J_{PH} = 3.7), 2.44 (dqn, 2H, CH_2, J_{PH} = 5.2, $^2J_{HH}$ = 13.7). A second CH_2 dqn is obscured by the CH_3 signal at δ 1.75. $^1H\{^{31}P\}$ NMR (CD_2Cl_2): δ 1.43 (s, 6H, CH_3), 1.60 (s, 6H, CH_3), 1.62 (s, 6H, CH_3), 1.75 (s, 6H, CH_3), 2.44 (d, 2H, CH_2, $^2J_{HH}$ = 13.7). A second CH_2 doublet is partially visible behind the CH_3 signal at δ 1.75. $^{31}P\{^1H\}$ NMR (CD_2Cl_2): δ −3.0 and −13.3 (AA′BB′ pseudotriplets). IR (Nujol): ν(CS) = 1011 cm^{-1} (literature value: 1010 cm^{-1}).[18] Anal. Calcd for $C_{11}H_{28}Cl_2P_4Pd_2S_2 \cdot 0.33\ CH_2Cl_2 \cdot 0.30\ Et_2O$: C, 22.26; H, 4.62; S, 9.37. Found: C, 21.97; H, 4.65; S, 9.70. The ^1H and $^{31}P\{^1H\}$ NMR data reported here are consistent with those reported previously.[13,18] Drying a sample of crystalline **5** at 78 °C in vacuo generated a mixture of **5**, **1a**, and **2a**, as determined by $^{31}P\{^1H\}$ NMR analysis of the resulting red solid.

In Situ Characterization of $Pd_2Cl_2(\mu\text{-CO})(depm)_2$. A solution of **1a′** in CD_2Cl_2 reacts with CO (1 atm) to yield an orange species that was characterized in situ by NMR spectroscopy. ^1H NMR (CD_2Cl_2): δ 0.96 (dqn, 2H, PCH_2P, J_{PH} = 4.5, $^2J_{HH}$ = 14.4), 1.21 (m, 24H, CH_3), 1.63 (dqn, 2H, PCH_2P, J_{PH} = 2.4, $^2J_{HH}$ = 14.4), 1.85 (m, 12H, CH_2CH_3), 2.36 (m, 4H, CH_2CH_3). $^1H\{^{31}P\}$ NMR (CD_2Cl_2): δ 0.96 (d, 2H, PCH_2P, $^2J_{HH}$ = 14.4), 1.20 (t, 12H, CH_3, $^2J_{HH}$ = 7.6), 1.22 (t, 12H, CH_3, $^2J_{HH}$ = 7.6), 1.63 (d, 2H, PCH_2P, $^2J_{HH}$ = 14.4), 1.80 (dq, 4H, CH_2CH_3, $^3J_{HH}$ = 7.2, $^2J_{HH}$ = 14.4), 1.89 (dq, 8H, CH_2CH_3, $^2J_{HH}$ = 15.6, $^3J_{HH}$ = 8.5), 2.36 (dq, 4H, CH_2CH_3, $^2J_{HH}$ = 15.6, $^3J_{HH}$ = 7.6). $^{31}P\{^1H\}$ NMR (CD_2Cl_2): δ 26.8 (s).

In Situ Characterization of $Pd_2Cl_2(\mu\text{-}CS_2)(depm)_2$ (5′). To a solution of **1a** (15 mg, 0.023 mmol) in CD_2Cl_2 (1 mL) was added CS_2 (0.050 mL, 63 mg, 0.829 mmol). Quantitative formation of **5′** was confirmed by $^{31}P\{^1H\}$ NMR spectroscopy. ^1H NMR (CD_2Cl_2): δ 1.02 to 1.29 (overlapping multiplets, 24H, CH_3), 1.67 (m, 2H, CH_2CH_3), 1.75 to 2.15 (overlapping multiplets, 14H, CH_2CH_3 and PCH_2P), 2.46 (m, 2H, CH_2CH_3), 2.59 (m, 2H, CH_2CH_3). $^1H\{^{31}P\}$ NMR (CD_2Cl_2): δ 1.08 (t, 6H, CH_3, $^3J_{HH}$ = 7.6), 1.16 (t, 6H, CH_3, $^3J_{HH}$ = 7.6), 1.20 (t, 12H, CH_3, $^3J_{HH}$ = 7.6), 1.23 (t, 6H, CH_3, $^3J_{HH}$ = 7.6), 1.67 (dq, 2H, CH_2CH_3, $^3J_{HH}$ = 7.1, $^2J_{HH}$ = 14.4), 1.75 to 2.15 (overlapping multiplets, 14H, CH_2CH_3 and PCH_2P), 2.46 (dq, 2H, CH_2CH_3, $^2J_{HH}$ = 15.8, $^3J_{HH}$ = 7.8), 2.60 (dq, 2H, CH_2CH_3, $^2J_{HH}$ = 15.8, $^3J_{HH}$ = 7.8). $^{31}P\{^1H\}$ NMR (CD_2Cl_2): δ 4.5, 16.1 (AA′BB′ pseudotriplets, apparent J_{PP} ∼16 Hz).

■ ASSOCIATED CONTENT

Supporting Information. X-ray crystallographic data for the structures of compounds **2a**, **2b**, and **5** (CIF files). Variable temperature $^{31}P\{^1H\}$ and ^1H NMR spectra of the $Pd_2Cl_2(depm)_2$ (**1a′**)/H_2S system. This material is available free of charge via the Internet at http://pubs.acs.org.

■ AUTHOR INFORMATION

Corresponding Author
*E-mail: brj@chem.ubc.ca.

Notes
[†]Deceased October 27, 1998.

■ ACKNOWLEDGMENT

We thank the Natural Sciences and Engineering Council of Canada for funding and Dr. T. Y. H. Wong for some initial investigations in this area. The reviewers of this paper are also thanked for their thoughtful comments.

■ REFERENCES

(1) (a) Mague, J. T. *J. Clust. Sci.* **1995**, *6*, 217. (b) Chaudret, B.; Delavaux, B.; Poilblanc, R. *Coord. Chem. Rev.* **1988**, *86*, 191. (c) Puddephatt, R. J. *Chem. Soc. Rev.* **1983**, 99.

(2) Besenyei, G.; Párkányi, L.; Gács-Baitz, E.; James, B. R. *Inorg. Chim. Acta* **2002**, *327*, 179 and refs cited therein.

(3) For representative examples, see: (a) Cera, M.; Cerrada, E.; Laguna, M.; Mata, J. A.; Teruel, H. *Organometallics* **2002**, *21*, 121. (b) Besenyei, G.; Párkányi, L.; Foch, I.; Simándi, L. I. *Angew. Chem., Int. Ed.* **2000**, *39*, 956. (c) Klopfenstein, S. R.; Kluwe, C.; Kirschbaum, K.; Davies, J. A. *Can. J. Chem.* **1996**, *74*, 2331. (d) Besenyei, G.; Lee, C.-L.; Gulinski, J.; Rettig, S. J.; James, B. R.; Nelson, D. A.; Lilga, M. A. *Inorg. Chem.* **1987**, *26*, 3622. (e) Olmstead, M. M.; Farr, J. P.; Balch, A. L. *Inorg. Chim. Acta* **1981**, *52*, 47.

(4) (a) Stockland, R. A., Jr.; Janka, M.; Hoel, G. R.; Rath, N. P.; Anderson, G. K. *Organometallics* **2001**, *20*, 5212 and refs cited therein. (b) Stockland, R. A., Jr.; Anderson, G. K.; Rath, N. P. *Inorg. Chim. Acta* **2000**, *300*−*302*, 395.

(5) Young, S. J.; Kellenberger, B.; Reibenspies, J. H.; Himmel, S. E.; Manning, M.; Anderson, O. P.; Stille, J. K. *J. Am. Chem. Soc.* **1988**, *110*, 5744.

(6) Kirss, R. U.; Eisenberg, R. *Inorg. Chem.* **1989**, *28*, 3372.

(7) Pamplin, C. B.; Rettig, S. J.; Patrick, B. O.; James, B. R. *Inorg. Chem.* **2003**, *42*, 4117.

(8) Hunt, C. T.; Balch, A. L. *Inorg. Chem.* **1981**, *20*, 2267.

(9) Wong, T. Y. H.; Rettig, S. J.; James, B. R. *Inorg. Chem.* **1999**, *38*, 2143.

(10) Richmond, M. K.; Scott, S. L.; Yap, G. P. A.; Alper, H. *Organometallics* **2002**, *21*, 3395.
(11) Pamplin, C. B. Ph.D. Thesis, The University of British Columbia, Vancouver, British Columbia, Canada, 2001.
(12) (a) James, B. R. *Pure Appl. Chem.* **1997**, *69*, 2213 and refs therein. (b) Barnabas, A. F.; Sallin, D.; James, B. R. *Can. J. Chem.* **1989**, *67*, 2009.
(13) Kullberg, M. L.; Kubiak, C. P. *Organometallics* **1984**, *3*, 632.
(14) Lee, C-Li.; Besenyei, G.; James, B. R.; Nelson, D. A.; Lilga, M. A. *J. Chem. Soc., Chem. Commun.* **1985**, 1175.
(15) Khorasani-Motlagh, M.; Safari, N.; Pamplin, C. B.; Patrick, B. O.; James, B. R. *Can. J. Chem.* **2006**, *84*, 330 and refs therein.
(16) (a) Bartholomew, C. H. *Appl. Catal., A* **2001**, *212*, 17 and refs therein. (b) Pietri, R.; Lewis, A.; Leon, R. G.; Casabona, G.; Kiger, L.; Yeh, S.-R.; Fernandez-Alberti, S.; Marden, M. C.; Cadilla, C. L.; Lopez-Garriga, J. *Biochemistry* **2009**, *48*, 4881 and refs therein.
(17) (a) Balch, A. L.; Benner, L. S.; Olmstead, M. M. *Inorg. Chem.* **1979**, *18*, 2996.(b) Balch, A. L. In *Homogeneous Catalysis with Metal Phosphine Complexes*; Pignolet, L. H., Ed.; Plenum Press: New York, 1983; p 183.
(18) Kullberg, M. L.; Kubiak, C. P. *Inorg. Chem.* **1986**, *25*, 26.
(19) Davies, J. A.; Kirschbaum, K.; Kluwe, C. *Organometallics* **1994**, *13*, 3664.
(20) Wink, D. J.; Creagan, B. T.; Lee, S. *Inorg. Chim. Acta* **1991**, *180*, 183.
(21) Stockland, R. A.; Anderson, G. K.; Rath, N. P. *Organometallics* **1997**, *16*, 5096.
(22) Atkins, P. W. *Physical Chemistry*; W. H. Freeman: Oxford, 1982; p 756.
(23) Wong, T. Y. H.; Barnabas, A. F.; Sallin, D.; James, B. R. *Inorg. Chem.* **1995**, *34*, 2278.
(24) Schwarz, D. E.; Dopke, J. A.; Rauchfuss, T. B.; Wilson, S. R. *Angew. Chem., Int. Ed.* **2001**, *40*, 2351.
(25) Wang, W.-D.; Guzei, I. A.; Espenson, J. H. *Inorg. Chem.* **2002**, *41*, 4780.
(26) Ma, E. S. F.; Rettig, S. J.; James, B. R. *Chem. Commun.* **1999**, 2463 and refs therein.
(27) Kullberg, M. L.; Lemke, F. R.; Powell, D. R.; Kubiak, C. P. *Inorg. Chem.* **1985**, *24*, 3589.
(28) (a) Ugo, R.; La Monica, G.; Cenini, S.; Segre, A.; Conti, F. *J. Chem. Soc. A* **1971**, 522.(b) Bogdanovic, B. Private communication; crystal structure for this complex published in 1992 in the Cambridge Crystallographic Database.
(29) Osakada, K.; Hayashi, H.; Maeda, M.; Yamamoto, T.; Yamamoto, A. *Chem. Lett.* **1986**, *4*, 597.
(30) Kuwata, S.; Hidai, M. *Coord. Chem. Rev.* **2001**, *213*, 211.
(31) (a) Maiti, K. M.; Görls, H.; Klobes, O.; Imhof, W. *Dalton Trans.* **2010**, *39*, 5713. (b) Boorman, P. M.; Moynihan, K. J.; Oakley, R. T. *J. Chem. Soc. Chem. Commun.* **1982**, 899.
(32) (a) Yamada, T.; Tanabe, M.; Osakada, K.; Kim, Y.-J. *Organometallics* **2004**, *23*, 4771. (b) Leoni, P.; Pasquali, M.; Sommovigo, M.; Laschi, F.; Zanello, P.; Albinati, A.; Lianza, F.; Pregosin, P. S.; Rüegger, H. *Organometallics* **1993**, *12*, 1702.
(33) (a) Tyree, W. S.; Vicic, D. A.; Piccoli, P. M.; Schultz, A. J. *Inorg. Chem.* **2006**, *45*, 8853. (b) Fryzuk, M. D.; Lloyd, B. R.; Clentsmith, G. K. B.; Rettig, S. J. *J. Am. Chem. Soc.* **1994**, *116*, 3804. (c) Fryzuk, M. D.; Clentsmith, G. K. B.; Leznoff, D. B.; Rettig, S. J.; Geib, S. J. *Inorg. Chim. Acta* **1997**, *265*, 169.
(34) Jennings, M. C.; Payne, N. C.; Puddephatt, R. J. *Inorg. Chem.* **1987**, *26*, 3776.
(35) Schlaf, M.; Lough, A. J.; Morris, R. H. *Organometallics* **1996**, *15*, 4423.
(36) Baxter, N. J.; Hosszu, L. L. P.; Waltho, J. P.; Williamson, M. P. *J. Mol. Biol.* **1998**, *284*, 1625 and refs therein.
(37) Jones, P. G.; Ahrens, B. *Chem. Commun.* **1998**, 2307.
(38) Fu, P. F.; Khan, M. A.; Nicholas, K. M. *Organometallics* **1993**, *12*, 3790.
(39) (a) Cameron, T. S.; Gardner, P. A.; Grundy, K. R. *J. Organomet. Chem.* **1981**, *212*, C19. (b) Pringle, P. G.; Shaw, B. L. *J. Chem. Soc., Dalton Trans.* **1983**, 889.
(40) Rosi, M.; Sgamellotti, A.; Tarantelli, F.; Floriani, C. *J. Organomet. Chem.* **1987**, *332*, 153.
(41) Pandey, K. K. *Coord. Chem. Rev.* **1995**, *140*, 37.
(42) Gaffney, T. R.; Ibers, J. A. *Inorg. Chem.* **1982**, *21*, 2860.
(43) Masciocchi, N.; Moret, M.; Sironi, A.; Ardizzoia, G. A.; Cenini, S.; LaMonica, G. *J. Chem. Soc., Chem. Commun.* **1995**, 1955.
(44) Datta, S.; Pandey, K. K.; Agarwala, U. C. *Inorg. Chim. Acta* **1980**, *40*, 65.
(45) Werner, H.; Bertleff, W. *Inorg. Chim. Acta* **1980**, *43*, 199.
(46) Hadj-Bagheri, N.; Puddephatt, R. J. *Inorg. Chem.* **1989**, *28*, 2384.
(47) Davies, J. A.; Dutremez, S.; Vilmer, M. *J. Prakt. Chem.* **1992**, *334*, 34.
(48) Balch, A. L.; Benner, L. S. *Inorg. Synth.* **1990**, *28*, 340.
(49) *d*TREK, Area Detector Software*, version 4.13; Molecular Structure Corp: The Woodlands, TX, 1996−1998.
(50) Altomare, A.; Burla, M. C.; Camalli, M.; Cascarano, G. L.; Giacovazzo, C.; Guagliardi, A.; Moliterni, A. G. G.; Polidori, G.; Spagna, R. *J. Appl. Crystallogr.* **1999**, *32*, 115.
(51) Sheldrick, G. M. *Acta Crystallogr.* **2008**, *A64*, 112.
(52) *WinGX*, V1.80.05; Farrugia, L. J. *J. Appl. Crystallogr.* **1999**, *32*, 837.
(53) *SQUEEZE*; Sluis, P. v. d.; Spek, A. L. *Acta Crystallogr., Sect. A* **1990**, *46*, 194.